Cancer Chemother Pharmacol (2008) 63:55–64
DOI 10.1007/s00280-008-0707-9

ORIGINAL ARTICLE

Does saturable formation of gemcitabine triphosphate occur in patients?

Lai-San Tham · Ling-Zhi Wang · Ross A. Soo · How-Sung Lee · Soo-Chin Lee · Boon-Cher Goh · Nicholas H. G. Holford

Received: 15 November 2007 / Accepted: 11 February 2008 / Published online: 28 February 2008

Abstract
Aim This study aims to determine if intracellular formation of gemcitabine triphosphate (dFdCTP), an active metabolite of gemcitabine, is saturable at doses used for treatment of Asian patients with lung cancer.
Methods From a phase II trial, plasma concentrations of gemcitabine, its inactive metabolite 2′-2′-difluorodeoxyuridine (dFdU), and mononuclear cell concentrations of gemcitabine-triphosphate were measured in 56 and 33 patients, respectively. The pharmacokinetics of gemcitabine and metabolites were modeled using nonlinear mixed effects modeling (NONMEM). A reduced dataset of ten randomly selected patients was employed to compare first-order and saturable formation of dFdCTP from gemcitabine.
Results The median population clearance estimate for dFdCTP formation with the full dataset was 70.2 L/h/70 kg/1.7 m. Modeling Michaelis–Menten formation of dFdCTP on a reduced dataset estimated K_m to be 3.6 times higher than the maximum gemcitabine concentration (72.2 μM) measured in this study.
Conclusions The results showed that first-order and nonsaturable clearance described intracellular dFdCTP formation at clinically applied doses of gemcitabine.

Keywords Gemcitabine · Gemcitabine triphosphate · Pharmacokinetics

Clinical Trial Registry: United States National Library of Medicine, NCT00212043.

L.-S. Tham · L.-Z. Wang · R. A. Soo · S.-C. Lee · B.-C. Goh
Department of Hematology–Oncology, National University Hospital, Singapore, Singapore

H.-S. Lee
Department of Pharmacology, Yong Loo Lin School of Medicine, National University of Singapore, Singapore, Singapore

N. H. G. Holford
Department of Pharmacology and Clinical Pharmacology, University of Auckland, Auckland, New Zealand

L.-S. Tham (✉)
Lilly-NUS Centre for Clinical Pharmacology Pte Ltd, Level 6, Centre for Clinical Research (MD11), National University of Singapore, Yong Loo Lin School of Medicine, 10 Medical Drive, Singapore, Singapore 117597
e-mail: tham_lai_san@lilly.com

Introduction

Gemcitabine (2′, 2′-difluorodeoxycytidine, dFdC) is a synthetic, cytotoxic agent that exhibits broad-spectrum activity against several solid tumors including lung, pancreatic, bladder, ovarian and breast cancers [12, 19]. Gemcitabine has a complex metabolic pathway. Gemcitabine is deaminated by cytidine deaminase both extracellularly and intracellularly to its main metabolite 2′, 2′-difluorodeoxyuridine (dFdU). Gemcitabine is transported into the cell and phosphorylated by deoxycytidine kinase (dCK) to its monophosphate (dFdCMP), and subsequently to its active diphosphate (dFdCDP) and triphosphate (dFdCTP) metabolites. Gemcitabine triphosphate is then incorporated into DNA inhibiting DNA polymerase, and DNA synthesis, as well as, masking DNA chain termination. Through multiple mechanisms of action gemcitabine is able to exhibit self-potentiation of cytotoxic activity [10, 14, 22, 23].

Two previous mass balance studies using radio-labeled gemcitabine reported somewhat differing urinary recovery of the drug and its metabolites. Storniolo et al.

reported 92–98% of the total dose was recovered within 1 week after administration of which 99% of the parent drug and dFdU was recovered in the urine and less than 1% was excreted via the feces [26]. Abbruzzese et al. described that a median of 77% (range 30–96%) of the administered dose was recovered in the urine within 24 h. The majority was eliminated within the first 6 h, of which a median of 5% was excreted as unchanged gemcitabine [1]. To date, few clinical studies have attempted to describe the relationship between plasma gemcitabine concentrations and intracellular dFdCTP (typically in blood mononuclear cells) [7, 8, 17, 20, 25, 29]. The method for measuring intracellular dFdCTP involves a delicate sample preparation process that includes the harvesting and counting of intact white bloods cells from freshly drawn blood samples.

Saturable formation of dFdCTP from gemcitabine has been postulated in both in vitro and in vivo reports. On the basis of the saturable formation hypothesis, it has been further suggested that the dosing of nucleoside analogues such as gemcitabine should most likely be based on the intracellular pharmacokinetics of their active metabolites because there may be a nonlinear relationship between plasma gemcitabine and its presumably active intracellular metabolite. Grunewald et al. conducted an in vitro study by incubating various concentrations of gemcitabine with leukemia cells harvested from four patients for 1 h, to demonstrate that increasing dFdC concentrations beyond 20 μM did not result in further intracellular formation of dFdCTP [7]. In two separate Phase I studies, Abbruzzese et al. and Grunewald et al. reported intracellular dFdCTP pharmacokinetics when gemcitabine was given over a range of increasing doses over 30 min. Peak concentrations in mononuclear cells did not increase further when plasma gemcitabine was above 20 μM. Large variability was observed in the peak concentrations and half-lives reported [1, 8]. In another phase I trial, Grunewald et al. reported a linear correlation between dFdCTP accumulation and increasing gemcitabine concentrations given over various infusion durations at 10 mg/m^2/min reaching peak dFdCTP concentrations of 17–2,235 μmol/L [9]. The median accumulation rate was 163 μM and saturation of dFdCTP was reported in 3 out of 22 patients, at intracellular concentrations of 350 and 750 μM at 2 h and 650 μM at 4 h. A previous report of our study suggested possible saturation in the study arm that was given gemcitabine at 1,000 mg/m^2 over 30 min but not in the 10 mg/m^2/min over 75 min arm [25]. Other reports have also examined possible schedule-dependence behavior of dFdCTP formation [30] and the effects of other co-administered anticancer agents [18]. Conclusions about the saturable formation of dFdCTP by graphical examination of drug concentrations are problematic. We conclude from this review of currently available literature that there is a lack of conclusive evidence from a quantitative pharmacology perspective for assuming that dFdCTP formation is saturable within the range of clinically applied doses of gemcitabine in patients. It will be important to determine if dFdCTP formation could be optimized using a fixed dose rate infusion regimen at 10 mg/m^2/min.

The primary objective of this study was to discern if a saturable or a first-order formation of dFdCTP better describes concentrations observed after clinically administered doses of gemcitabine. The secondary objective of this study is to identify covariates that may predict variability in the clearance of gemcitabine and its metabolites in Asian lung cancer patients.

Methods

Data

The gemcitabine, dFdU plasma concentrations and dFdCTP intracellular concentrations used in this study were collected prospectively from a randomized controlled, phase II trial aimed at comparing the effects of gemcitabine infused at a fixed dose rate of 750 mg/m^2 over 75 min (10 mg/m^2/min, $n = 28$) versus 1,000 mg/m^2 over 30 min ($n = 28$), given on days 1 and 8 every 3 weeks in Asian stage IIIB or IV, non-small cell lung cancer patients [25]. Carboplatin dose was administered as a 1 h infusion just prior to gemcitabine on day 1 of every cycle, to patients in both treatment arms based on a target carboplatin area under the concentration (AUC) time curve of 5 min mg/mL. The study protocol was approved by the Domain Specific Review Board and a signed informed consent obtained from all patients prior to participation in this study.

Blood samples were drawn on day 1 of cycle 1 based on the following protocol times: baseline, 10, 30 min into the infusion, 10 min before the end of infusion, 30, 60 and 120 min following completion of the infusion. At each sampling, 10 mL of venous blood were drawn of which 2 mL was sent for a differential full blood count at the National University Hospital's Department of Laboratory Medicine and the remaining 8 ml was drawn into heparinized tubes pre-loaded with tetrahydrouridine, a cytidine deaminase inhibitor to prevent ex vivo conversion of gemcitabine to dFdU. After separating plasma by centrifugation, peripheral mononuclear cells were isolated immediately from the remaining buffy coat via Ficoll-Hypague PLUS density gradient centrifugation (Amersham Biosciences, Sweden). Cell pellets were washed and suspended in 6 ml PBS for counting. After centrifugation, the final cell pellets in PBS was adjusted

as 100 μL and stored in freezer (−80°C) until HPLC analysis. Patients who did not manage to have their blood samples drawn on day 1 of cycle 1 had their blood samples taken at subsequent cycles of chemotherapy. Actual infusion and sampling times were recorded for pharmacokinetic modeling purposes. Because of potential discrepancies between clinical records of infusion duration and measured concentrations it was decided to try to estimate the variability around the recorded infusion duration.

Reference standards for bioanalysis of gemcitabine, dFdU and dFdCTP were provided by Eli Lilly and Company. Analysis of plasma samples for determining dFdC and dFdU concentrations were performed by an isocratic ion-pair reversed phase high performance liquid chromatography (HPLC) method [34]. Intracellular dFdCTP concentrations were determined by a gradient anion-exchange high performance liquid chromatography (HPLC) assay modified from Heinemann et al. [11]. HONE1 cell line was used as control biological matrix because of difficulty in obtaining human white blood cells. Samples containing 2 million cells were extracted with perchloric acid and neutralized with potassium hydroxide before HPLC analysis. Good specificity was achieved as no endogenous peaks co-eluted with dFdCTP in all patients' blank cells. The limit of detection was 0.2 μM. Good linearity was achieved for concentration range of 0.4–10 μM with $r^2 > 0.998$. Three QC samples showed recovery to be >90%. The intraday and interday precision was 2–4 and 7–11%, respectively. Accuracy ranged 87–108%. All validations complied with FDA guidance for industry bioanalytical method validation (http://www.fda.gov/cder/Guidance/4252fnl.pdf). The amount of dFdCTP determined in mononuclear cells was corrected for the number of mononuclear cells in the sample and by the mean cell volume of each sample. The assumption made was that dFdCTP was uniformly distributed among all the cells in each sample.

Computation

Computation of population pharmacokinetics parameter estimates was performed using nonlinear regression (NONMEM version VI release 1.1; GloboMax LLC, Hanover, MD, USA). The first-order conditional estimation (FOCE) method with interaction was applied to derive population pharmacokinetic parameter estimates, between subject variability (BSV) and residual unexplained variance (RUV) from observed concentrations. The Intel Visual Fortran compiler (Version 9.1) was used to compile NONMEM with options/nologo/nbs/w/4Yportlib/Gs/Ob1gyti/Qprec_div.

Pharmacokinetic model

Gemcitabine and its intracellular metabolite, dFdCTP, were initially fitted simultaneously using subroutines from the NONMEM library (Fig. 1a). The estimated population parameters were gemcitabine volumes of distribution for the central (V_{1G}) and peripheral (V_{2G}) compartments, intercompartmental gemcitabine clearance (Q), and gemcitabine clearance into the intracellular compartment to form dFdCTP (CL_{G2T}). Volume of distribution at steady state (Vss) for gemicitabine was reported based on the summation of V_{1G} and V_{2G}. Subsequently, the extracellular

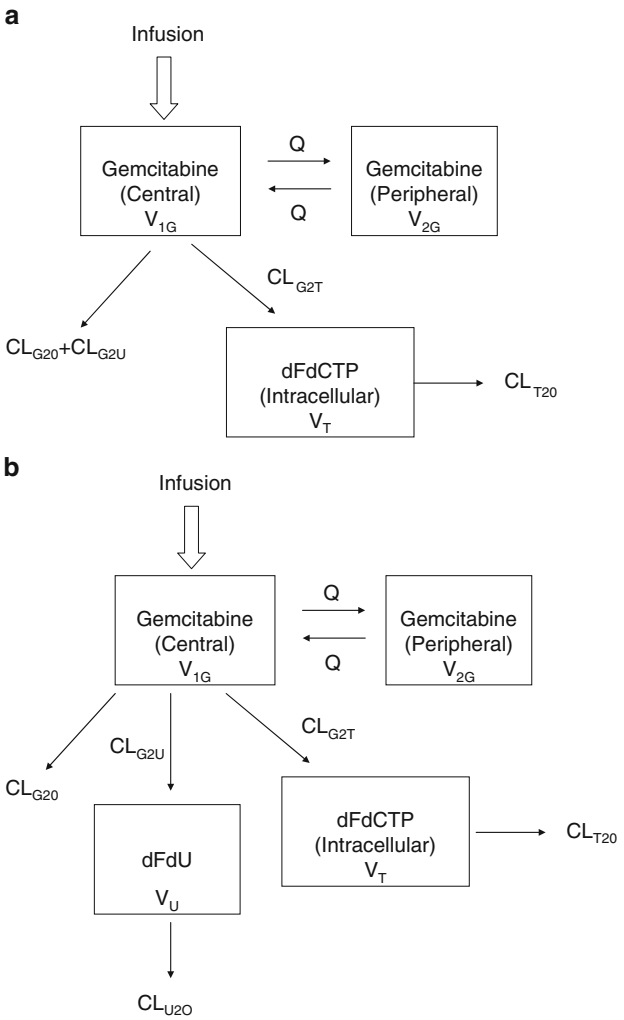

Fig. 1 **a** Structural model of gemcitabine and dFdCTP. *Q* intercompartmental clearance; CL_{G2O} gemcitabine clearance; CL_{G2U} gemcitabine clearance (dFdU formation); CL_{G2T} gemcitabine clearance (intracellular dFdCTP formation); CL_{T2O} dFdCTP clearance; V_{1G} gemcitabine volume of distribution in central compartment; V_{2G} gemcitabine volume of distribution in peripheral compartment; V_T dFdCTP volume of distribution; **b** Structural model of gemcitabine and dFdCTP with dFdU. CL_{U2N} non-renal clearance of dFdU; CL_{U2R} renal clearance of dFdU; V_U dFdU volume of distribution

metabolite, dFdU, was added to the data and all concentrations were fitted simultaneously. Clearance of unchanged gemcitabine, CL_{G2O}, and clearance to dFdU, CL_{G2U} were predicted from CL_{G2T} by assuming the fractional conversion of gemcitabine into the respective metabolites reported from a mass-balance study by Abbruzzese et al. [1]. In that study, 77% of radioactive gemcitabine was recovered in the urine of which a median of 5% was being excreted as unchanged gemcitabine. Hence, the remainder of the drug that was unaccounted for was assumed to have been phosphorylated intracellularly to dFdCTP. Therefore, the fraction of gemcitabine converted to dFdCTP was assumed to be 23% (F2T). The fraction of gemcitabine excreted unchanged was assumed to be 4% (F2O) and this leaves the fraction deaminated by cytidine deaminase to dFdU as 73% (F2U). Thus total clearance of gemcitabine, CL_G was predicted from CL_{G2T}/F2T, CL_{G2O} from $CL_G \times$ F2O and CL_{G2U} from $CL_G \times$ F2U. This parameterization of clearance was chosen in order to make it simpler to test a mixed order process for formation of dFdCTP.

Two models were compared to describe formation of dFdCTP. These were either a first order conversion of gemcitabine to dFdCTP (CL_{G2T}) or a mixed order conversion $\frac{V_{max,G2T}}{K_m+C}$. V_{max} is the maximum conversion rate in μmol/h/70 kg/1.76 m, K_m is the Michaelis–Menten constant in μM and C is gemcitabine concentrations in μM. CL_G, CL_{G2O} and CL_{G2U} were computed during solution of the differential equations using the value of CL_{G2T} predicted from $\frac{V_{max,G2T}}{K_m+C}$ at each gemcitabine concentration. Because of the extensive computational time associated with the solution of the full Michaelis–Menten model based on differential equations (ADVAN 6), a reduced dataset of ten randomly selected patients with 60 gemcitabine, 60 dFdU and 40 dFdCTP observations was used.

By adopting a sequential fitting approach, using the population pharmacokinetic parameters and data (PPP&D) method, the estimates for a gemcitabine model were fixed before the dFdU compartment was added [36]. The best estimates from this sequential model were then employed as the initial estimates for a simultaneous fit of the model to concentrations from all three compounds.

Model selection was based on changes of the NONMEM's objective function value (ΔOBJ) and visual predictive checks. A decrease in objective function value (ΔOBJ) of >3.84 ($P < 0.05$) was considered statistically significant for the addition of a fixed effect ($df = 1$). The final model was evaluated using a non-parametric bootstrap and a visual predictive check. The visual predictive check assesses the adequacy of the model when it is used to simulate the median and 90% prediction interval and compared to the corresponding median and 90% observation interval obtained at similar times.

Predictable sources of between subject variability

In order to examine possible relationships between gemcitabine and its metabolites with patient characteristics, the covariates recorded and used for fitting included, age, body size, Karnofsky performance status (KPS), NSCL cancer staging of IIIB or IV, creatinine clearance, sex, race, and smoking history. Creatinine clearance for a standard 70 kg patient was calculated from serum creatinine concentrations and creatinine production rate based on the Cockcroft–Gault formula. Renal function (RF) was calculated as the ratio of predicted creatinine clearance standardized to 70 kg, to the nominal standard of 100 ml/min/70 kg. A new size descriptor, normal fat weight (NFWT) was compared with actual body weight to account for differences in size and body composition. Standardized NFWT (SNFWT) is a derivative of body size centered on a standard individual with a weight of 70 kg and height of 1.76 m. The derivation of NFWT is as follows:

Derivation of normal fat weight for an individual:

$$\text{Lean body mass in kg, LBM} = \text{LBM}_{MAX} \times \text{HT}^2 \times \frac{\text{WT}}{(\text{WT}_{50} + \text{WT} \times \text{HT}^2)} \quad (1)$$

$$\text{Normal fat weight in kg, NFWT} = \text{LBM} + \text{FFAT} \times (\text{WT} - \text{LBM}) \quad (2)$$

where LBM_{MAX} are lean body mass and maximum lean body mass in kg, respectively, HT is height in cm, WT and WT_{50} are actual weight and 50% of maximum actual weight in kg, respectively. FFAT is a representation of the fat fraction in the body.

Derivation of normal fat weight for a standard subject with height 1.76 m and weight 70 kg:

$$\text{Lean body mass for standard subject in kg, LBM}_{STD} = \text{LBW}_{MAX} \times 1.76^2 \times \frac{70}{(\text{WT}_{50} + 70 \times 1.76^2)} \quad (3)$$

$$\text{Normal fat weight for standard subject in kg, NFWT}_{STD} = \text{LBM}_{STD} + \text{FFAT} \times (70 - \text{LBM}_{STD}) \quad (4)$$

Derivation of the size descriptor: standard normal weight, which is centered on 1 based on ratio of Eqs. 2 to 4,

$$\text{Standard normal fat weight, SNFWT} = \frac{\text{NFWT}}{\text{NFWT}_{STD}} \quad (5)$$

Standard weight computed from total body weight divided by 70 kg or SNFWT was then used in an allometric model to predict between subject differences in clearance and volume parameters [13].

In addition, covariates were fitted into the model in a stepwise approach. Categorical variables, treated as

dichotomous, and continuous variables were tested as follows:

$$\text{Categorical: } CL = CL_{POP} \cdot (1 + \text{covariate}_{effect}) \quad (6)$$

$$\text{Continuous: } CL = CL_{POP} \cdot \exp(\text{covariate}_{effect} \cdot (\text{covariate} - \text{median})) \quad (7)$$

where CL_{POP} is population clearance and median is the median value for the covariate being tested.

Total gemcitabine clearance adjusted for covariate values was predicted as follows:

$$CL_{G,GRP} = (CL_{GRP,G2T} + CL_{GRP,G2U} + CL_{GRP,G2O}) \quad (8)$$

where CL_{GRP} is the group value of each clearance component obtained after accounting for covariate effects. CL_{G2T} is gemcitabine clearance to dFdCTP, CL_{G2U} is the clearance of dFdU and CL_{G2O} is the clearance of unchanged gemcitabine.

Random sources of between subject variability

The random effect for between subject variability (BSV) of any gemcitabine clearance was described using an exponential model such as the one showed for CL_{G2T}:

$$CL_{G2T} = CL_{GRP,G2T} \cdot \exp(BSV_{CL,G2T}) \quad (9)$$

where $BSV_{CL,G2T}$ is the between subject variability estimate for gemcitabine clearance to dFdCTP.

Similar exponential functions were used for BSV of other parameters.

Residual unexplained variability

Residual unidentified variability (RUV) was described by assuming a combined model with proportional and additive normal distributions of random differences of the observations from the predictions.

Between subject parameter variability in the residual error model was estimated for each observation by obtaining THETA estimates of proportional (RUV_CV) and additive (RUV_SD) residual error parameters. Random between subject differences in RUV ($\eta_{PPV\_RUV,i}$) were obtained by estimating its variance (PPV_RUV,*i*) [15]. The ε random effect was fixed with a unit variance.

$$SD = \text{sqrt}\left(\left(C_{i,j} \cdot \theta_{RUV\_CV}\right)^2 + \left(\theta_{RUN\_SD}\right)^2\right) \cdot \exp\left(\eta_{PPV\_RUV,i}\right)$$

$$Y_{i,j} = C_{i,j} + SD \cdot \varepsilon$$

Bootstrap confidence interval

In the final step, a non-parametric bootstrap method with replacement was used to construct confidence intervals (CIs) for the uncertainty of the parameters. Re-sampling was repeated 1,000 times and the 5th and 95th percentiles of the bootstrap parameter estimates were used to define the 90% confidence intervals for each parameter estimate.

Results

Patients

A total of 327 plasma gemcitabine and 328 plasma dFdU concentrations from 56 patients and 180 intracellular dFdCTP concentrations from 33 patients were utilized for pharmacokinetic modeling. Patient demographics for all 56 subjects who were included in this study as listed in Table 1. The majority (83.9%) of the patients were diagnosed to as having stage IV non-small cell lung cancer.

Pharmacokinetics of gemcitabine and intracellular gemcitabine 5′-triphosphate (dFdCTP) and 2′-2′-difluorodeoxyuridine (dFdU)

In the initial structural model consisting of just gemcitabine and dFdCTP (Fig. 1a), the standard normal fat weight (SNFWT) size descriptor was found to be better than allometric scaling ($\Delta OBJ = -25.68$, $df = 4$) which was

Table 1 Patient characteristics

	Mean
Age, in years (±SD)	58.2 ± 9.7
Sex	
Male	39
Female	17
Race	
Chinese	45
Malays	10
Indians	0
Others	1
Cancer staging	
IIIB	9
IV	47
Karnofsky performance status	
70–80%	11
90–100%	45
Weight in kg (±SD)	58.1 ± 11.9
Height in m (±SD)	1.61 ± 0.08
CLcr in ml/min (±SD)	74.7 ± 18.9
Smoking history	
Current smoker	10
Ex-smoker	21
Non-smoker	25

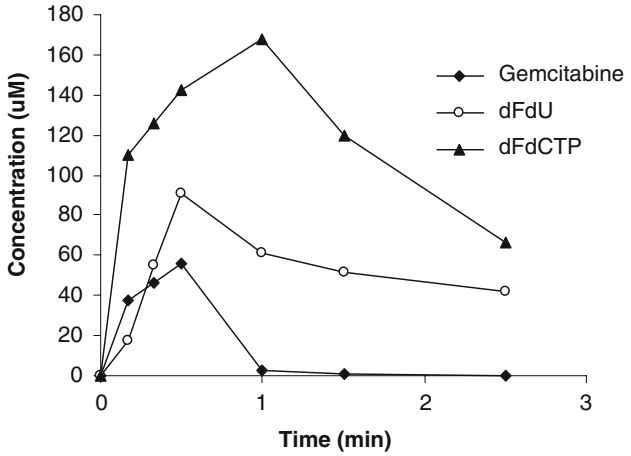

Fig. 2 The concentration-time profiles of gemcitabine (*solid circles*) and dFdU (*open circles*) in plasma and dFdCTP (*solid triangles*) in white blood cells from a typical patient

better than a base model without a size descriptor (ΔOBJ $= -15.7$, $df = 1$). In this size descriptor model, the fat fraction of body composition was estimated to be zero, thereby reducing the size descriptor as equivalent to the lean body mass, a derivation of height and weight. Inclusion of other covariates did not show significant improvements in the model.

The concentration-time profiles of gemcitabine and dFdU in plasma, versus intracellular concentrations of dFdCTP in a typical patient is depicted in Fig. 2. The median of the final estimates for the pharmacokinetic parameters, their between subject variabilities and 90% confidence intervals obtained from 1,000 runs in the bootstrap method are listed in Table 2. From the bootstrap, the median values for mean residence time (MRT) of gemcitabine in the central compartment and total gemcitabine clearance (CL_G) with standard deviation were to be 0.17 h and 305.2 ± 13.8 L/h/70 kg/1.76 m, respectively. The median values of the proportional and additive standard deviations of the hybrid model for residual unexplained variability were 0.35 and 0.03 μmol/L for gemcitabine, 0 and 35.9 μmol/L for dFdCTP and, 0.15 and 4.09 μmol/L for dFdU.

The Michaelis–Menten model conducted on a reduced dataset of ten patients did not produce an objective function value lower than that of a first-order model for dFdCTP formation from gemcitabine fitted to the same dataset. The Michaelis–Menten constant, K_m and maximum conversion rate, V_m, values obtained were 263 μM/h and 23800 μM/70 kg/1.76 m, respectively. The concentrations for gemcitabine in this study ranged from 0.027 to 72.24 μM.

Discussion

Using a population pharmacokinetic modeling technique, the final model adequately characterized the pharmacokinetic profiles of gemcitabine and its metabolites. The final estimate for total gemcitabine clearance, derived from the summation of all routes of gemcitabine elimination in this model was 305.2 ± 13.8 L/h/70 kg/1.76 m. This value was comparable to the values reported for Chinese patients in a small study of six patients (236.4 ± 40.3 L/h) as well in the Western population (153–244.8 L/h) [28]. Due to the complexity of gemcitabine's metabolic pathway, reports on the pharmacokinetic parameters of its metabolites have been scarce. In the only other paper that adopted a multi-compartmental approach to describe gemcitabine and dFdU pharmacokinetics, Venook et al. reported dFdU clearance of 5.57 L/h in a cohort of patients with hepatic or

Table 2 Median values, 90% confidence intervals and between subject variability of pharmacokinetic parameters from bootstrapping of the final model

Variables	Parameters	Estimates (90% CI)[a]	Between subject variability (90% CI)[a]
Body size descriptor	FFAT	0	Fixed
Gemcitabine	Vss (L/70 kg/1.76 m)	51.3 (43.7, 59.8)	Fixed
	MRT (h)	0.17 (0.1, 0.2)	Fixed
	Q (L/h/70 kg/1.76 m)	156 (124, 201)	0.3 (0.05, 0.4)
	CL_{G2T} (L/h/70 kg/1.76 m)	70.2 (65.3, 75.7)	0.3 (0.2, 0.4)
	V_{1G} (L/70 kg/1.76 m)	2.96 (0.20, 7.8)	2.4 (1.6, 4.9)
	V_{2G} (L/70 kg/1.76 m)	47.6 (41.3, 56.4)	0.1 (0.001, 0.2)
	CL_{G2U} (L/h/70 kg/1.76 m)	222.8 (207.2, 240.3)	Fixed
	CL_{G2O} (L/h/70 kg/1.76 m)	12.2 (11.4, 13.2)	Fixed
	CL_G (L/h/70 kg/1.76 m)	305.2 (283.9, 329.1)	Fixed
dFdCTP	CL_{T2O} (L/h/70 kg/1.76 m)	3.0 (2.6, 3.4)	0.4 (0.3, 0.5)
	V_T (L/70 kg/1.76 m)	4.6 (4.1, 5.1)	0.4 (0.3, 0.5)
dfdU	CL_{U2O} (L/h/70 kg/1.76 m)	21.5 (19.8, 23.5)	0.3 (0.2, 0.4)
	V_U (L/70 kg/1.76 m)	52.6 (49.3, 55.9)	0.3 (0.2, 0.3)

[a] 90% CI reported where applicable

renal dysfunction. The corresponding dFdU clearance from this study of patients with renal and hepatic function values within normal laboratory limits was 21.5 L/h/70 kg/1.76 m or 7% of total gemcitabine clearance. No other reports of dFdCTP pharmacokinetic parameters exist to date [30]. Since the relative formation of dFdU and dFdCTP from gemcitabine was not directly identifiable in this study, assumptions were made based on estimates from a radioactive metabolic profiling study of gemcitabine to allow estimation of plausible values for the pharmacokinetic parameters [1].

Model adequacy was checked using a visual predictive check method through simulating 150 datasets and comparing the median and prediction intervals of gemcitabine and its metabolites from these simulations with the actual observations (Fig. 3). In most parts, the median values and 90% prediction intervals of the simulated concentrations for gemcitabine and dFdU were very close to that of the median values and 90% observation intervals of the observed concentrations although dFdCTP concentrations appeared less well predicted. We attribute this to the smaller number of observations that were available for dFdCTP.

A comparison of the objective function values from the reduced dataset of ten patients showed that a first-order model for dFdCTP formation from gemcitabine fitted the data as well as the Michaelis–Menten model. Since K_m far exceeds C_{max} in the Michaelis–Menten model, we can

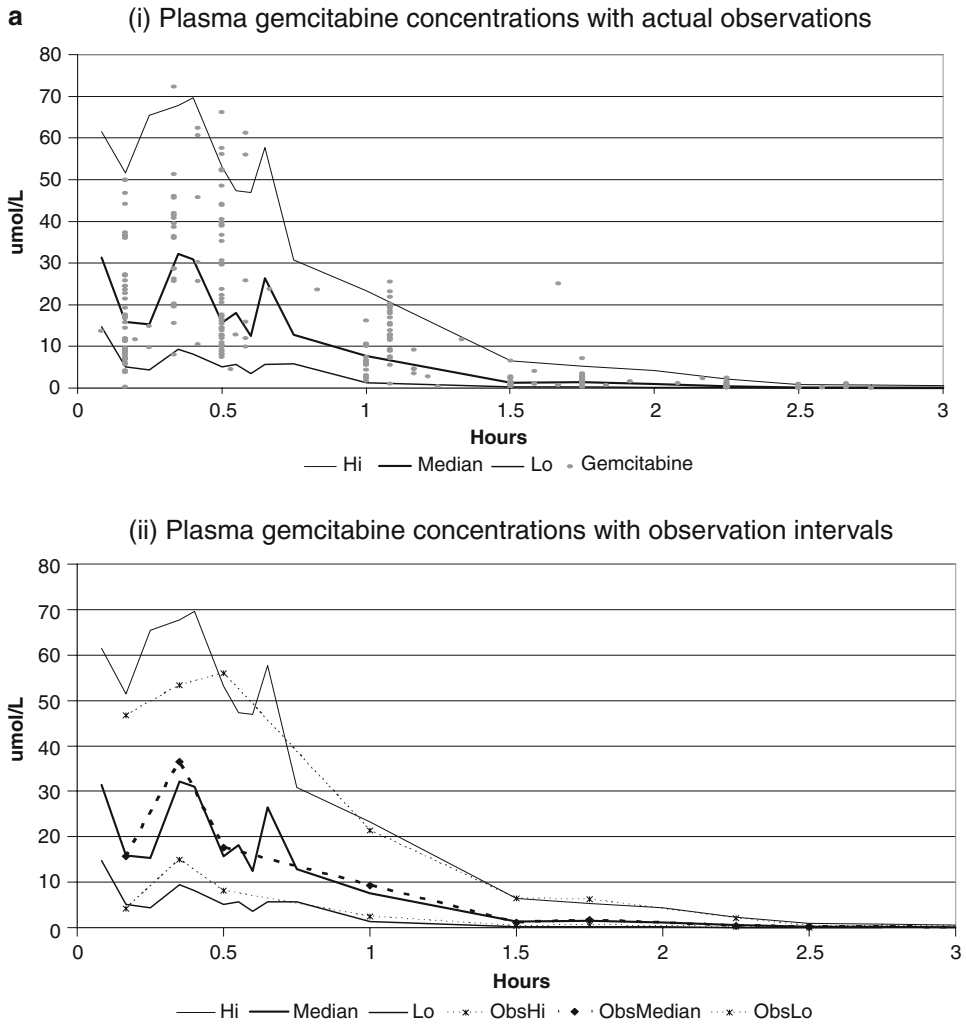

Fig. 3 **a** Visual predictive check of gemcitabine concentrations using 150 simulated datasets over a study period of 3 h. Plots of (i) observed concentrations (*grey dots*), simulated median concentration (*thick solid line*) and its 90% prediction intervals (*thin solid line*) of simulated dataset; (ii) median values of observed concentrations (*perforated solid line*) and that of its 90% observation intervals (*thin perforated lines*) versus median (*thick solid line*) and 90% predicted intervals (*thin solid lines*) of simulated datatset. **b** Visual predictive check of dFdU concentrations (symbols are similar to Fig. 3a, c). Visual predictive check of dFdCTP concentrations (symbols are similar to Fig. 3a)

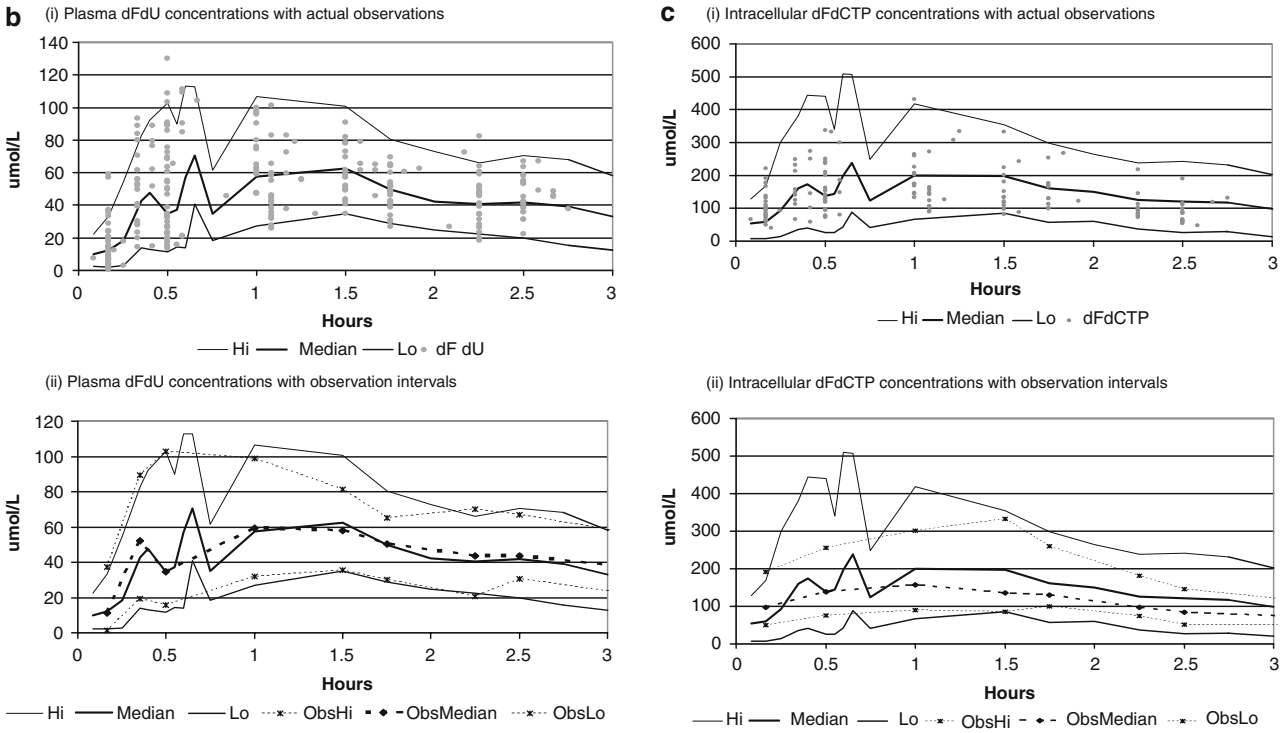

Fig. 3 continued

conclude that within the clinically used doses of gemcitabine in this study, there is no evidence to support saturable formation of dFdCTP. The maximum gemcitabine concentration achieved in our study (72.2 μM) was comparable to the mean peak concentrations achieved in clinical studies by Abbruzzese et al. and Grunewald et al. at similar doses [1, 9]. Since the K_m value we have estimated was above gemcitabine concentrations achieved with clinical doses administered in this study, the evidence supports a linear relationship between plasma gemcitabine and dFdCTP at steady state. It should be noted that the intracellular dFdCTP concentrations, which ranged from 39.7 to 431.4 μM, were performed in mononuclear white cells. There are some ex vivo evidence to suggest that these cells are not representative of the target tumour cells in terms of mechanism and rate and extent of conversion of gemcitabine to dFdCTP [20]. In addition, since saturation of dFdCTP formation was not achieved, the results of this modelling approach supports our previous clinical observations that patients who received the fixed dose rate infusion of 75 mg/m^2 for 75 min and 1,000 mg/m^2 over 30 min showed comparable clinical effectiveness and safety profile [25]. It may be necessary to re-examine the effects of infusion duration for fixed dose rate regimens.

From this study, the covariates that predicted differences in clearance were weight and height. In an abstract by Allerheiligen et al., they reported that age, gender, body surface area and duration of infusion influenced the disposition of gemcitabine [2]. Although age was tested in this model, the range was narrower in our study, ranging from 39 to 74 years old compared to 29 to 78 years in Allerheiligen's study. After accounting for body size using the size descriptor, standard normal fat weight, (SNFWT) instead of body surface area, we found that sex could not further explain variability in gemcitabine clearance. Allometric scaling has been widely used for predicting human pharmacokinetics based on animal data. Its application in population pharmacokinetics modeling is also becoming increasingly useful. In the typical allometric model, the "3/4 power law" is applied to a standard weight descriptor [13, 21, 27, 28, 35] more often being either the actual body weight or lean body weight. Body surface area (BSA), derived from body weight and height, via the Du Bois and Du Bois formula, is commonly applied in oncology and pediatric dosing of drugs. This appears to be just a tradition that has spread from routine clinical practice, despite criticisms on its lack of adequate validation [3]. Other size descriptors, such as predicted normal weight, have been evaluated in obese populations [5, 6, 15]. In our study, we compared actual body weight and SNFWT for allometric scaling in our model. Interestingly, the SNFWT size descriptor has an estimated fat fraction that was zero, reducing it to just lean body mass. This confirmed that the fat content of the body can be ignored when choosing an effective size descriptor for gemcitabine.

Our study offers further understanding of gemcitabine metabolism, in particular the pharmacokinetics of its main metabolites. We have successfully modeled the pharmacokinetics of gemcitabine and its metabolites. The other reported active diphosphate metabolite (dFdCDP) of gemcitabine was not studied for the reasons that its effects cannot be distinguished from the major and more active triphospahte metabolite (dFdCTP) and dFdCTP remained the most commonly reported active metabolite of gemcitabine. In addition, since this study was performed in combination with carboplatin, which is of the same pharmacological class as cisplatin, and the latter has been shown to influence dFdCTP accumulation in patients and tumor cells, the effects of carboplatin on gemcitabine pharmacokinetics were not distinguishable from this model [3, 30, 31]. Nevertheless, this model does serve to pave the way for investigating possible explanations of pharmacokinetics variability by genetic polymorphisms, demographics or other environmental factors by testing the covariate effects of these factors in appropriate pathways within this model. This may in turn provide some explanation for between subject variability in drug response.

Conclusions

The results of this study identified lean body mass as an important size descriptor having an effect on the pharmacokinetics of gemcitabine and its metabolites. We have tested the hypothesis that saturable formation of dFdCTP from gemcitabine occurs when gemcitabine was given in clinically used doses. The time course of concentrations of gemcitabine and its major metabolites give no support for saturable formation with these doses and administration rates used in the current study.

Acknowledgments This work was supported by grants from the Biomedical Research Council (BMRC 01/1/26/18/060), Singapore Cancer Syndicate (SCS PN0022) and Eli Lilly and Company.

References

1. Abbruzzese JL, Grunewald R, Weeks EA, Gravel D, Adams T, Nowak B, Mineishi S, Tarassoff P, Satterlee W, Raber MN (1991) A phase I clinical, plasma, and cellular pharmacology study of gemcitabine. J Clin Oncol 9:491–498
2. Allerheiligen S, Patel B, Dhahir P, Johnson R, Hatcher B, Cerimele B, Rugg T, Tarassoff P, Dorr A (1995) Population pharmacokinetic analyses: effect of age, gender, duration of infusion, body surface area on gemcitabine pharmacokinetics. Pharm Res 12(Suppl 1):S327
3. Bergman AM, Ruiz van Haperen VW, Veerman G, Kuiper CM, Peters GJ (1996) Synergistic interaction between cisplatin and gemcitabine in vitro. Clin Cancer Res 2:521–530
4. Du Bois D, Du Bois EF (1916) A formula to estimate the approximate surface area if height, weight be known. Arch Intern Med 17:863–871
5. Duffull SB, Dooley MJ, Green B, Poole SG, Kirkpatrick CM (2004) A standard weight descriptor for dose adjustment in the obese patient. Clin Pharmacokinet 43:1167–1178
6. Green B, Duffull SB (2004) What is the best size descriptor to use for pharmacokinetic studies in the obese? Br J Clin Pharmacol 58:119–133
7. Grunewald R, Kantarjian H, Keating MJ, Abbruzzese J, Tarassoff P, Plunkett W (1990) Pharmacologically directed design of the dose rate and schedule of 2′,2′-difluorodeoxycytidine (Gemcitabine) administration in leukemia. Cancer Res 50:6823–6826
8. Grunewald R, Abbruzzese JL, Tarassoff P, Plunkett W (1991) Saturation of 2′,2′-difluorodeoxycytidine 5′-triphosphate accumulation by mononuclear cells during a phase I trial of gemcitabine. Cancer Chemother Pharmacol 27:258–262
9. Grunewald R, Kantarjian H, Du M, Faucher K, Tarassoff P, Plunkett W (1992) Gemcitabine in leukemia: a phase I clinical, plasma, and cellular pharmacology study. J Clin Oncol 10:406–413
10. Heinemann V, Xu YZ, Chubb S, Sen A, Hertel LW, Grindey GB, Plunkett W (1992) Cellular elimination of 2′,2′-difluorodeoxycytidine 5′-triphosphate: a mechanism of self-potentiation. Cancer Res 52:533–539
11. Heinemann V, Hertel LW, Grindey GB, Plunkett W (1988) Comparison of the cellular pharmacokinetics and toxicity of 2′,2′-difluorodeoxycytidine and 1-beta-D-arabinofuranosylcytosine. Cancer Res 48:4024–4031
12. Hertel LW, Boder GB, Kroin JS, Rinzel SM, Poore GA, Todd GC, Grindey GB (1990) Evaluation of the antitumor activity of gemcitabine (2′,2′-difluoro-2′-deoxycytidine). Cancer Res 50:4417–4422
13. Holford NH (1996) A size standard for pharmacokinetics. Clin Pharmacokinet 30:329–332
14. Huang P, Chubb S, Hertel LW, Grindey GB, Plunkett W (1991) Action of 2′,2′-difluorodeoxycytidine on DNA synthesis. Cancer Res 51:6110–6117
15. Janmahasatian S, Duffull SB, Ash S, Ward LC, Byrne NM, Green B (2005) Quantification of lean bodyweight. Clin Pharmacokinet 44:1051–1065
16. Karlsson MO, Jonsson NE, Wiltse CG, Wade JR (1998) Assumption testing in population pharmacokinetic models: illustrated with an analysis of moxonidine data from congestive heart failure patients. J Pharmacokinet Biopharm 26(2):207–246
17. Kroep JR, Giaccone G, Voorn DA, Smit EF, Beijnen JH, Rosing H, van Moorsel CJ, van Groeningen CJ, Postmus PE, Pinedo HM, Peters GJ (1999) Gemcitabine and paclitaxel: pharmacokinetic and pharmacodynamic interactions in patients with non-small-cell lung cancer. J Clin Oncol 17:2190–2197
18. Kuenen BC, Rosen L, Smit EF, Parson MR, Levi M, Ruijter R, Huisman H, Kedde MA, Noordhuis P, van der Vijgh WJ, Peters GJ, Cropp GF, Scigalla P, Hoekman K, Pinedo HM, Giaccone G (2002) Dose-finding and pharmacokinetic study of cisplatin, gemcitabine, and SU5416 in patients with solid tumors. J Clin Oncol 20:1657–1667
19. Noble S, Goa KL (1997) Gemcitabine. A review of its pharmacology, clinical potential in non-small cell lung cancer and pancreatic cancer. Drugs 54:447–472
20. Peters GJ, Clavel M, Noordhuis P, Geyssen GJ, Laan AC, Guastalla J, Edzes HT, Vermorken JB (2007) Clinical phase I and pharmacology study of gemcitabine (2′, 2′-difluorodeoxycytidine) administered in a two-weekly schedule. J Chemother 19:212–221
21. Peters RH (1983) The ecological implications of body size. Cambridge University Press, Cambridge
22. Plunkett W, Huang P, Searcy CE, Gandhi V (1996) Gemcitabine: preclinical pharmacology and mechanisms of action. Semin Oncol 23(Suppl 10):3–15

23. Plunkett W, Huang P, Xu YZ, Heinemann V, Grunewald R, Gandhi V (1995) Gemcitabine: metabolism, mechanisms of action, and self-potentiation. Semin Oncol 22(Suppl 11):3–10
24. Sawyer M, Ratain MJ (2001) Body surface area as a determinant of pharmacokinetics and drug dosing. Invest New Drugs 19:171–177
25. Soo RA, Wang LZ, Tham LS, Yong WP, Boyer M, Lim HL, Lee HS, Millward M, Liang S, Beale P, Lee SC, Goh BC (2006) A multicentre randomised phase II study of carboplatin in combination with gemcitabine at standard rate or fixed dose rate infusion in patients with advanced stage non-small-cell lung cancer. Ann Oncol 52:153–158
26. Storniolo AM, Allerheiligen SR, Pearce HL (1997) Preclinical, pharmacologic, and phase I studies of gemcitabine. Semin Oncol 24(Suppl 7):S7-2–S7-7
27. Tang H, Mayersohn M (2005) A novel model for prediction of human drug clearance by allometric scaling. Drug Metab Dispos 33:1297–1303
28. Tang H, Mayersohn M (2005) Accuracy of allometrically predicted pharmacokinetic parameters in humans: role of species selection. Drug Metab Dispos 33:1288–1293
29. Tempero M, Plunkett W, Ruiz Van Haperen V, Hainsworth J, Hochster H, Lenzi R, Abbruzzese J (2003) Randomized phase II comparison of dose-intense gemcitabine: thirty-minute infusion and fixed dose rate infusion in patients with pancreatic adenocarcinoma. J Clin Oncol 21:3402–3408
30. van Moorsel CJ, Kroep JR, Pinedo HM, Veerman G, Voorn DA, Postmus PE, Vermorken JB, van Groeningen CJ, van der Vijgh WJ, Peters GJ (1999) Pharmacokinetic schedule finding study of the combination of gemcitabine and cisplatin in patients with solid tumors. Ann Oncol 10:441–448
31. van Moorsel CJ, Pinedo HM, Veerman G, Bergman AM, Kuiper CM, Vermorken JB, van der Vijgh WJ, Peters GJ (1999) Mechanisms of synergism between cisplatin and gemcitabine in ovarian and non-small-cell lung cancer cell lines. Br J Cancer 80:981–990
32. Venook AP, Egorin MJ, Rosner GL, Hollis D, Mani S, Hawkins M, Byrd J, Hohl R, Budman D, Meropol NJ, Ratain MJ (2000) Phase I and pharmacokinetic trial of gemcitabine in patients with hepatic or renal dysfunction: cancer and leukemia group B 9565. J Clin Oncol 18:2780–2787
33. Wang LR, Huang MZ, Xu N, Shentu JZ, Liu J, Cai J (2005) Pharmacokinetics of gemcitabine in Chinese patients with non-small-cell lung cancer. J Zhejiang Univ Sci B 6:446–450
34. Wang LZ, Goh BC, Lee HS, Noordhuis P, Peters GJ (2003) An expedient assay for determination of gemcitabine and its metabolite in human plasma using isocratic ion-pair reversed-phase high-performance liquid chromatography. Ther Drug Monit 25:552–557
35. West GB, Brown JH, Enquist BJ (1997) A general model for the origin of allometric scaling laws in biology. Science 276:122–126
36. Zhang L, Beal SL, Sheiner LB (2003) Simultaneous vs. sequential analysis for population PK/PD data I: best-case performance. J Pharmacokinet Pharmacodyn 30:387–404